JPIChE 48 (1) 2020: 49-56

PAKISTAN INSTITUTE OF CHEMICAL ENGINEERS
Since 1969

Journal of Pakistan Institute of Chemical Engineers

journal homepage: www.piche.org.pk/journal

Highly Efficient Zinc Oxide Nanostructure Based Gas Sensor For Domestic Application

R. Khan[1], M.N. Khan1[1], M. Amin[1], S. Siddiqui[2], S.H. Sultan[1], B.K. Kasi[3], G. Malghani[4], S.K. Sami[1]*

Submitted: 11/02/2018, Accepted: 21/03/2018, Online: 26/04/2018

Abstract

In present work, high surface to volume ratio Zinc Oxide (ZnO) nanorods were fabricated by hydrothermal synthesis on a glass slide and highly conductive alumina ceramic based gold interdigitated electrode (IDE). Developed nanorod structure and growth was characterized by X-ray diffraction (XRD), UV absorption spectroscopy and Scherrer's equation, respectively. The sensitivity characterization of fabricated sensor was determined for 2000 ppm and 4000 ppm natural gas in the air through high resistance electrometer at room temperature. The 2000 ppm concentration of gas shows 11.3% sensitivity at response time of 66 seconds and recovery time of 92 seconds to the sensor. The 4000 ppm concentration of gas shows 64% sensitivity, the response time of 106 seconds and a recovery time of 174 seconds to the sensor. The higher sensitivities with slow response and recovery times exhibit the behavior of redox reactions of sensor surface to the higher concentration of natural gas. The more concentration of natural gas in the air would show a higher sensitivity of the sensor. The experimental results indicate the growth of ZnO nanorods on substrates and their sensitivity to natural gas.

Keywords: *Zno nanorods, Fabrication, Hydrothermal, Gas sensor; Sensitivity, XRD*

1. Introduction:

In casting process, there are number of parameters

Natural gas is a highly used combustible gas in domestic and commercial sectors and have higher British thermal unit (BTU) that ranges from 850 to 1050 per cubic feet [1]. Worldwide estimated reserves of natural gas are hundreds of trillion cubic meters [2]. In Pakistan 757 billion cubic meter proven reserves of natural gas are available to meet the energy demand and most of the gas produced is supplied through the pipeline by government distribution companies [1]. However, the combustion of natural gas is causing environmental pollution due to release of NOx and Sox [3]. In Pakistan, many people lost their lives during winter season due to the unsafe use of natural gas as a heat source on the domestic level. These losses of life and environmental effects need the detection of gas leakage before it crosses its lower explosive limit (LEL). The presence of these gases in the atmosphere with little concentration is dangerous. Therefore, very sensitive gas sensors with high accuracy are necessary for domestic and industrial sector.

The gas sensors devices can be effectively applied for gas leakage detection by transferring the

[1] *Department of Chemical Engineering, Balochistan University of Information Technology, Engineering and Management Sciences,* Quetta,
[2] *Department of Textile Engineering, Balochistan University of I.T., E. & Management Sciences, Quetta, Pakistan*
[3] *Department of Computer Engineering, Balochistan University of I.T., E. & Management Sciences, Quetta, Pakistan*
[4] *Department of Environmental Sciences, Balochistan University of I.T., E. & Management Sciences, Quetta, Pakistan*
***Corresponding Author:** kamran.sami@buitms.edu.pk

chemical information to an electrical signal in the form of frequency, voltage or current changes [4]. Fundamentally an alarm is a resonance to warn the people as the leakage of toxic gases is sensed by the gas sensors before the permissible exposure limit crosses i.e. at a very low concentration of toxic/hazard gases [5]. Various types of sensors have been developed depending on their application range and efficiency i.e. catalytic, thermal conductive, electrochemical, optical and semiconductor gas sensors. Among these the semiconductor based sensors gained increased interest owing to their high efficiency and accuracy. In the semiconductor gas sensors, the resistance or conductance change of the device is measured by electrometer after the interaction of target gas with metal oxide semiconductors surface [4]. The semiconductor gas sensor is developed after the fabrication of synthesized metal oxide nanoparticles mostly ZnO, SnO_2, WO_3 or ln_2O_3 on the interdigitated substrate. On the surface of metal oxide nanostructure, the reversible gas adsorption process takes place with target gas which is said to be chemical signals. These chemical signals transferred to electrical signals by electrodes on a substrate. The change in resistance is measured by a high resistance electrometer [6]. If a redox reaction did not take place on the surface of the sensor while interacting with a sensor with target gas or in the recovery time of the sensor, then a heater needed to speed up the reaction. These nanoparticles of metal oxides are synthesized in such nanostructures which allow adsorption and/or reaction of the target gas in very less time on its surface that changes conductance/resistance. The occurrence of increase or decrease in resistance largely depends on the target gas (i.e. the gas is oxidizing or reducing) and type of metal oxide semiconductor (i.e. n-type or p-type semiconductor) [4, 6]. ZnO is found to be an attractive metal oxide because of its improved sensitivity, selectivity and stability after effective doping process and its easy fabrication as a thin and thick film [6, 7]. ZnO is a II-VI type semiconductor compound that has a bandgap of 3.4 eV (at 300 K), the resistivity of 10^{74} to 10^{12} cm and a melting point of 2240?C. The ZnO having a large surface to volume ratio, with low heat transfer and a density of 5.67 [8]. This one-dimensional ZnO film includes nanoribbons, Nano needles, nanofiber mats, Nano-whiskers, nanowire, Nano belts, nanotubes and nanorod. Due to the high length to diameter ratio of these nanostructures appropriately sense the target gas [9]. The ZnO nanorods with its 2-20 nm length to diameter ratio can be synthesized by different methods.

It is important to characterize the growth of metal oxide nanorods before it is exposed to target gas for sensing parameters. Nanorods' growth can be characterized through XRD and UV spectroscopy. S.A. Vanalakar in 2018 followed the hydrothermal synthesizing method to grow nanorods on the glass substrate and characterized it through XRD. The main instance peak of (002) plane exhibited the growth of ZnO in a perpendicular position to the substrate. When the concentration of the zinc nitrate has increased the peak on the 2è position of (002) plane also increases with the minor improvement of (100) plane too [10]. ZnO Nanorods growth in different concentration of zinc nitrate in ZnO crystal growth solution with various growth temperatures showed peaks on 2è position with Bragg plane of (100), (002) and (101) indicate the hexagonal crystal system of ZnO Nanorods [11]. The optical properties of a material are highly dependent on its nanostructure. The result for a higher bandgap of semiconductor metal oxide mostly shows its absorption peak below 400 nm wavelength. Pijus Kanti Smanata presented that absorption spectrum in the UV region of ? 372 nm wavelength is showing the growth of ZnO nanorods [12].

The ZnO thin film with a palladium catalyst layer was chemically fabricated on the substrate to find out its response time, sensitivity and recovery time by using methane gas. The sensor shows its optimum result of 84% sensitivity on 200?C in 1%V of methane in the air [13]. In another study, the highest sensitivity of 84% for 2600 ppm of LPG by Pd coated ZnO nanorods conducting substrate sensor and 70% sensitivity for 5000 ppm of LPG by

un-coated ZnO nanorods at 100°C was reported [14]. Although, there are some studies dealing with ZnO based gas sensors but nanoparticles formation and fabrication way can greatly affect the efficiency of sensor and needs to be further investigated. Hence, this work is focused on (1) development of ZnO particles and their hydrothermal synthesis (2) characterization and application for gas sensing (3) Performance evaluation for gas leakage detection.

2. Materials and Methods:

2.1 Chemicals:

The chemical used were of analytical grade and were purchased from United Traders, Quetta.

2.2. Nanoparticles Synthesis Process:

The hydrothermal synthesis process is found to be a promising procedure for the synthesis of nanostructures (Fig. 1). The Gold Interdigitated Electrode Alumina Ceramic and glass slide substrates were immersed in soap solution and sonicated for 20 minutes in a water bath sonicator for cleaning. The substrates were thoroughly washed with DI water and sonicated with acetone for another 20 minutes. The 1mM Zn acetate in 60 ml of ethanol were prepared for seeding. The aluminum sheet was placed on Hotplate and substrates with perfect horizontal alignment were arranged. The hot plate was set on 150°C and the 100µl seeding solution on the substrates was dropped for the four times through 1 mL pipette tip and the substrates were cooled down to room temperature. The crystallization process was executed in Carbolite Gero ELF 11/6B furnaces by putting substrates in aluminum sheets.

In crystallization the furnaces incubating temperature was set on 350°C. In ZnO crystal growth solution preparation initially, the 20mM Zn nitrate solution in 200 mL DI water was prepared than a 20mM Hexamine solution in 200 mL DI water was prepared. After that mixed both the solution in a beaker and finally volume of 400mL would yield an equimolar 10mM solution of both Zn nitrate and hexamine was obtained. A clean Petri-dish and a scotch tape was used by sticking substrates and keaped the seeded layer of the substrate downwards face. The Petri-dish was filled with crystal growth solution and incubated for 30 mints in the micro oven by keeping the power of the micro oven on 2. This ZnO nanorods growth procedure was repeated five times after discarding the solution and replaced it with a fresh crystal growth solution. After the completion of nanorods growth the substrates were gently washed it with DI water. The substrates were arranged on an aluminum tray and anneal it at 250°C for 1 hour. Lastly, the substrates were allowed to cool down to room temperature.

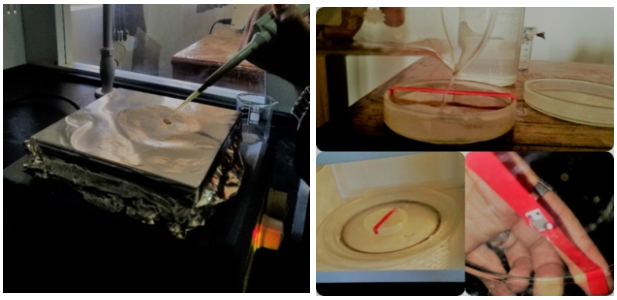

Figure1: ZnO particles seeding and growth process

2.3. Gas Sensor Characterization Process:

This procedure describes the characterization of nanostructured metal oxide semiconductor-based gas sensors using the test bench. The change in resistance of the ZnO nanorods fabricated Gold IDE alumina ceramic substrate was found out through a 6517A high resistance electrometer when the sensor was exposed to 2000 ppm and 4000 ppm of natural gas in the air. The schematic of the test setup for the gas sensor characterization is shown in Fig. 2. The test bench comprises of the gas delivery system, sensor test chamber and sensor response measurement system. The gas delivery system includes an Air pump, natural gas flow measuring setup, gas flow-lines and pressure regulators. The test chamber contains the glass tube with a 2.5 inch internal diameter and a thermocouple and heat controller. However, the sensor response measurement system includes ZnO nanorods fabricated Gold IDE alumina ceramic substrate sensor that is connected to 6517A high resistance electrometer through soldered wires for

resistance measurement. While performing the experiments always wear safety glasses, lab coat, hand gloves and facemask for protection from harmful gases and chemicals. Ensure that the connection with Gold IDE is proper with no loose connections. Due to loose connections, the resistance on electrometer will show high fluctuation before test startup which needs a soldering job with gold IDE sensor and electrometer probes.

Figure 2: Gas sensor test bench for characterization of gas.

3. Results and Discussion:

3.1 ZnO Nanords Characterization:

The UV absorption spectroscopy characterization was executed through Ultra-3660 UV-VIS Spectrophotometer. Before fabrication on Alumina ceramic based Gold IDE the hydrothermal synthesis process mentioned in chapter 3 was exercised on a glass slide. The UV absorption spectroscopy results of ZnO nanorods on glass slides show its absorption peak at 372 nm and higher absorption peak at 293nm wavelength as shown in Fig 3, which depicts the growth of ZnO nanorods on a glass slide. ZnO nanorods with its higher bandgap showed its highest absorption peak at a short wavelength of 293 nm that exhibits broadband absorption in the UV band. The hydrothermal synthesis was further applied to Alumina ceramic based Gold IDE. The UV absorption spectroscopy results of ZnO nanorods fabricated Alumina based Gold IDE sensor show its strong absorption peak at 369 nm and extended the absorption peak to 315 nm wavelength shown in Fig 4. The fluctuation was seen in extension region of Fig 4 from absorption peak of 369 nm to 315nm was due to ZnO nanorods fabrication on Alumina ceramic based Gold IDE substrate. The result exhibited that the Zinc Oxide nanorod containing higher bandgap were more active in the shorter wavelength of the ultraviolet region that shows a broadband absorption of the sensor. Moreover, these results are consistent with literature information as well.

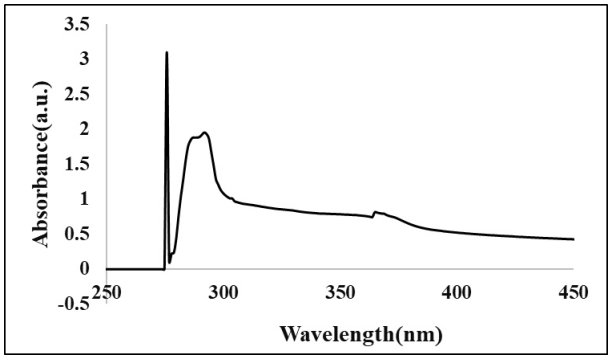

Figure 3: UV absorption spectroscopy results ZnO nanorods Fabricated glass side

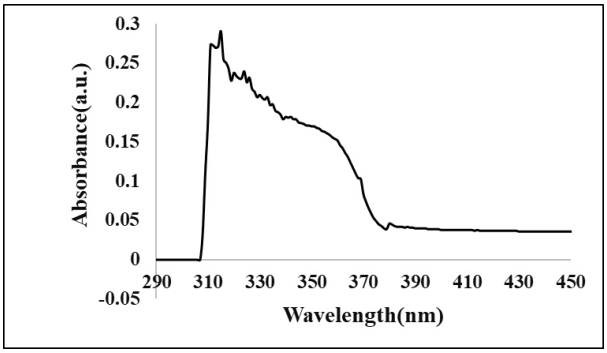

Figure 4: UV absorption spectroscopy results ZnO nanorods Fabricated Gold IDE

3.2 XRD Analysis:

The XRD intensity peaks of ZnO nanorods fabricated substrates were observed through the X-ray Diffraction 2D Phaser. The XRD 2D phaser was operated on 10 mA current and 30 KeV voltage and the Gonio scanning axis was adopted with a range of scanning from 7.99 2è to 80.79 2è at room temperature. The Cu-Ká was used for radiation at a lambda of 1.54184 ?A. Initially, the hydrothermal synthesis process was executed on a glass slide. The XRD results of ZnO nanorods on the glass slide is

were run and three samples were obtained from each trial. After preparation of 24 samples as shown in Figure 5, ultimate tensile strength of samples on MTS machine was analyzed. 3 values

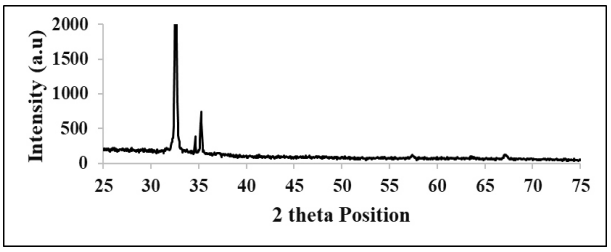

Figure 5: XRD of ZnO nanorods Fabricated on Glass slide

The main instance peak of (002) plane exhibited the growth of ZnO in a perpendicular position to the substrate. The ZnO nanorods peaks show its maximum peak intensity of (002) Bragg plane on 34.85? and showing peaks on (100), (101), (102), (110), (200), (112) and (202) Bragg planes. The three main peaks on 2è position with Bragg plane of (100), (002) and (101) indicate the hexagonal crystal system of ZnO nanorods. The XRD result of Zinc oxide nanorods fabricated on Gold IDE Alumina Ceramic substrate 90% agrees with J.C.P.D.S standard (Card No: 71-1123), (Card No: 36-1451) and (No: 04-0784) as shown in Figure 6 for Alumina Ceramic, ZnO nanorods and Gold respectively. This exhibits that the ZnO nanorods are in hexagonal wurtzite vertical position i.e. perpendicular to the substrate.

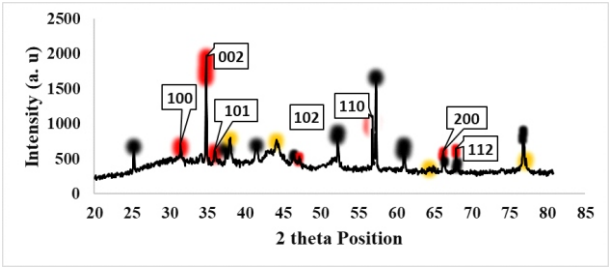

Figure 6: XRD of ZnO Nanorods Fabricated on Gold IDE Alumina Ceramic substrate.

3.3 Zinc Oxide Nanorods Size Determination:

X-ray diffraction technique was used to identify the size of ZnO nanorods. Debye-Scherrer's equation was used to determine the average crystal size of ZnO nanorods from XRD peaks of ZnO nanorods. It was used for both XRD peaks of ZnO nanorods fabricated on a glass slide and highly conductive Alumina ceramic based Gold IDE substrates.

Scherrer's Formula:

$$Dp \quad K \; / \; \cos \qquad (1)$$

Where Dp is the crystallite size in nanometer (nm), K is Scherrer constant, is the wavelength of X-ray, is the full width at half maximum (FWHM) and is the one half of 2 position of XRD peak. The Scherrer equation relates the crystallite size in a solid to the XRD peak width . Its purpose is to calculate the size of the crystal in the solid. The crystallite shape factor K in Scherrer equation varies from 0.8 to 1.2, however, its average value was taken in crystallite size determination such as 0.94. In the calculation, the X-ray wavelength ë was taken from XRD raw data which was 1.54184?A. The FWHM (value) was calculated from OrigionPro 64-bit software for each peak of ZnO nanorods from XRD data of ZnO nanorods fabricated on substrates is shown in Table 4.1 and Table 4.2. The angle was determined by taking one half of 2 position on Bragg's plane (100) 32.6°, (002) 34.6° and (101) 35.3° for ZnO nanorods on a glass substrate. However, for ZnO nanorods on Gold IDE substrate, one half of 2 position on Bragg's plane (100) 31.5°, (002) 34.8°, (101) 35.9°, (102) 47.1°, (110) 56.9°, (200) 66.2° and (112) 67.9° was taken for angle determination. The average size of ZnO nanorods on a glass substrate and Alumina ceramic based Gold IDE substrate were determined from equation 3 of different XRD peaks as shown in Table 1.

Table 1: Crystallite size of ZnO nanorods

Sample	Bragg's plane (hkl)	2è position	FWHM (â)	Crystal size Dp (nm)
Crystallite size of ZnO nanorods on a glass substrate	100	32.6°	0.215	40.24
	002	34.6°	18.08	0.48
	101	35.3	0.17	51.25

Table 1: Crystallite size of ZnO nanorods

Sample	Bragg's plane (hkl)	2è position	FWHM (â)	Crystal size Dp (nm)
Crystallite size of ZnO nanorods on a glass substrate	100	32.6°	0.215	40.24
	002	34.6°	18.08	0.48
	101	35.3°	0.17	51.25
	Average Crystal size Dp 31 nm			
Crystallite size of ZnO nanorods on Alumina ceramic based Gold IDE substrate.	100	31.5°	0.673	12.88
	002	34.8°	0.164	54.39
	101	35.9°	26.45	0.33
	102	47.14°	122.77	0.07
	110	56.85°	0.156	60.53
	200	66.22°	0.23	43.10
	112	67.9°	0.101	99.1
	Average Crystal size Dp 38.6 nm			

The highest peak on the 2 position of ZnO nanorods on glass substrate showed a crystal size of 40.24 nm. On (002) and (101) 2 positions it showed crystal size of 0.48 nm and 51.24 nm respectively. The average crystallite size obtained from Scherrer's equation for ZnO nanorods fabricated on the glass substrate was 31 nm. The results of Debye-Scherrer's equation for glass substrate exhibited that the size of fabricated ZnO nanorods was the size of nanorods. The crystallite size of 54.39 nm, 60.53 nm, 43.10 nm and 99.11 nm for the higher peaks (002), (110), (200) and (112) on 2 positions respectively of ZnO nanorods on Gold IDE substrate with its average crystallite size of 38.6 nm verify the growth of nanorods. Lastly, the average crystallite size of 31 nm and 38.6 nm of ZnO nanorods on a glass slide and Gold IDE substrate shows that the ZnO nanorods hydrothermal synthesis exhibited a growth of ZnO nanorods.

3.4 Sensitivity Characterization to Natural Gas:

The aim of study was to sense the natural gas before it reaches to its lowest explosive limit (i.e. 4.4% V in air) and lowest occupational explosive limit (i.e. 5300 ppm) at 10% of its lowest explosive limit (Prasad, Saurabh., et al 2011) (JP Hodges, W Geary., et al 2015). The synthesis of ZnO nanorods on Gold IDE Alumina Ceramic substrate is for the purpose to characterize the sensing tendency for natural gas to ZnO nanorods. During the characterization, the key value of the experiment was to obtain resistance of the sensor at any point of time from the inserting to the ejecting of natural gas in the test chamber. The resistance was found through a 6517A high resistance electrometer with the applied source through electrometer of 9volt. As the natural gas with 88% of methane gas is reducing gas when it interacts with fabricated ZnO nanorods sensor. The oxidation reaction took place on the surface of the sensor and the gain of electrons due to oxidation reaction reduces the resistance of the sensor. This resistance at the time of sensor exposer to 2000 ppm concentration of natural gas in the air was recorded. The resistance of the sensor in the Air was 2200 k which was reduced when the natural gas was supplied to the test chamber. In the 2000 ppm concentration of natural gas, the resistance reduces to 1947 k as shown in Fig 7. After the lowest stationary resistance, the gas supply was terminated and the increase in the resistance was recorded. In the 4000 ppm concentration of natural gas, the higher reduction in the resistance was recorded. During the supply of a higher concentration of natural gas, the resistance stationary on its lowest value of 800 k for 14 seconds. At this stage, the further supply of natural

gas was stopped and the increase in the resistance was recorded. These resistance values on specific timing during sensor exposer to 2000 ppm and 4000 ppm were changed to the percentage of the sensitivity to gas. The sensitivity (%) was obtained from the equation:

$$\text{Sensitivity (\%)} = \frac{R_a - R_g}{R_a} \times 100 \qquad (2)$$

Where Ra is resistance in the air however Rg is resistance in gas. The sensitivity (%) versus time graph is shown in Figure 4.8 depicts the sensitivity change when the sensor was exposed to natural gas in the presence of air. When 2000 ppm concentration natural gas is supplied to the test chamber sensor show its highest sensitivity at 11.3% for 8 seconds and its response time was 66 seconds however the sensor recovery time was 92 seconds. On the other hand, when the same sensor was exposed to 4000 ppm concentration it took more time to fully respond to natural gas i.e. 64% sensitivity which remains stable for 14 seconds. During the exposer of a sensor to 4000 ppm concentration of gas, the response time was 106 seconds and the recovery time was 174 seconds as shown in Table 2.

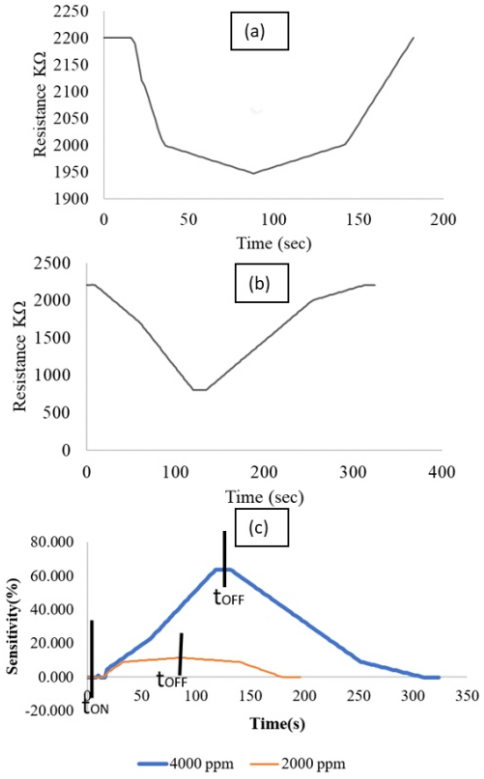

Figure 7: The Resistance change pattern during sensor exposer to (a) 2000 ppm (b) 4000 ppm of natural gas and (c) Sensitivity (%) of ZnO nanorods Fabricated on Gold IDE to natural gas

Table 2: ZnO nanorods sensor sensing properties.

Natural Gas Concentration	Sensitivity (%)	Response time (sec)	Recovery time (sec)
2000 ppm	11.3%	66	92
4000 ppm	64%	106	174

The lower concentration of natural gas becomes quickly stabled showing minute sensitivity of 11.3%. It is because of the lower concentration of gas which hardly reduces the resistance of the sensor. The lower concentration with lower recovery time after the closing of the supply of natural gas to the test chamber shows the quick reduction reaction of the air with a sensor surface. The higher concentration responds slowly but with a higher sensitivity of 64% which indicates the slow oxidation reaction at the sensor surface. However, the higher concentration exceedingly reduces the resistance of the sensor by taking more time than the lower concentration of gas.

P. Mitra synthesize ZnO thin film with a Palladium catalyst layer through chemical deposition method to sense methane gas. The author supplies 10000 ppm (1% V) of methane gas in air to test chamber and observed the sensor sensing properties in different temperature from 100°C to 300°C. However, the optimum sensitivity of 84% and lowest R_{Gas}/R_{Air} (ratio of resistance in gas to resistance in Air) were observed under the temperature of 200°C with the sensor response and recovery time of 10 mints as shown in figure 4.9. Musarrat Jabeen sense another reducing gas LPG through Pd doped ZnO nanowires and ZnO nanorods on Aluminum foil fabricated through solvothermal process which shows sensitivity of 84% and 70% respectively. The sensor exhibits the response time of 100 seconds and recovery time of 240 seconds in 2600 ppm concentration of LPG in Air under the temperature of 100°C. The ZnO nanorods fabricated on highly conductive Alumina

ceramic based Gold IDE shows fine sensitivity of 64% and better response time and recovery time to reducing gas (natural gas) in room temperature of 106 sec and 174 sec respectively, as compare to other higher temperature-based gas sensors. The ZnO nanorods and thin film fabricated on Aluminum foil and glass slide respectively, which show well sensitivity but with higher response and recovery time in higher temperature environments

4. Conclusions:

In this study, the Zinc oxide nanorods were successfully fabricated on Alumina ceramic based Gold interdigitated electrode and glass slide substrate. That was confirmed after the characterization of ZnO nanorods growth through XRD and UV absorption spectroscopy results. The XRD intensity peaks and UV absorption spectroscopy absorption peak was obtained from X-ray diffraction 2d phaser and Ultra-3660 UV-VIS Spectrophotometer. The XRD pattern was compared with JCPDS standards of ZnO nanorods, Gold and Alumina ceramic. The XRD pattern was further used for crystallite size determination through Scherrer's equation. Crystallite size determination further verifies the ZnO nanorods growth by its crystallite size result of 38.6 nm and 31 nm for ZnO nanorods on Gold IDE and glass substrates respectively. The obtained UV absorption peak was compared with the previous results in the literature review of ZnO nanorods absorption peaks (as mentioned in section 2.4.1), which confirmed the growth of ZnO nanorods. For the characterization of sensing properties, the sensor was soldered with a 6517A high resistivity electrometer. The resistance after applying 9volt voltage was obtained by keeping the sensor in the test chamber such that in the environment of a specific concentration of natural gas with 88% methane in the air. The sensor showed the 2200 kÙ resistance in air and 2000 ppm and 4000 ppm concentration of natural gas, it showed its lowest resistance of 1947 kÙ and 800 kÙ respectively. In 2000 ppm of natural gas in the air, the sensor shows 11.3% sensitivity with 66 seconds of response time and 92 seconds of recovery time to natural gas. However, in 4000 ppm the natural gas shows 64% sensitivity, 106 seconds response time and 174 seconds recovery time to target gas.

References:

1. Organization of Petroleum Exporting Countries (OPEC), 2017, Online Annual Statistical Bulletin 2017. Online Annu Stat Bull 2017 217
2. H. Devold, "Oil and Gas Production Handbook - An introduction to oil and gas production", 2002.
3. M. Amin et al., "Bioenergy production from waste mango seed shell by thermo-chemical conversion and its importance for mango fruit processing industry", *Journal Buitms Edu Pk,* 1:4852, 2019.
4. Y. Min, "Properties and Sensor Performance of Zinc Oxide Thin Films", *Ceramics,* 2003.
5. Z. Yunusa, M. N. Hamidon, A. Kaiser, Z. Awang, "Gas sensors: A review", *Sensors and Transducers,* 2014.
6. T. Thabothanayakam, "Synthesis and Characterization of Zinc Oxide and Tin Oxide Based Nanostructures for Gas Sensing Applications", *Thesis Submitted in Fulfilment of the Requirements for the Degree of Doctor of Philosophy Faculty of Engineering University of Malaya*, 165, 2015.
7. S. K. Sami et al., "The Pine-Needle-Inspired Structure of Zinc Oxide Nanorods Grown on Electrospun Nanofibers for High-Performance Flexible Supercapacitors", *Small*, doi: 10.1002/smll.201702142, 2017.
8. Y. J. Chen et al., "Synthesis and enhanced gas sensing properties of crystalline CeO 2/TiO2 core/shell nanorods", *Sensors Actuators B Chem,*. doi: 10.1016/j.snb.2011.02.057, 2011,
9. M. M. Arafat, B, Dinan, S. A. Akbar, A. Haseeb, "Gas sensors based on one dimensional nanostructured metal-oxides: A review", *Sensors,* (Switzerland), 2012.
10. S. A. Vanalakar et al., "Enhanced Gas-Sensing Response of Zinc Oxide Nanorods Synthesized

via Hydrothermal Route for Nitrogen Dioxide Gas", *J Electron Mater*. doi: 10.1007/s11664-018-6752-1, 2019.

11. I. K. R. Laila, et al., "Synthesis and Characterization of ZnO Nanorods by Hydrothermal Methods and Its Application on Perovskite Solar Cells", *Journal of Physics: Conference Series,* 2018.
12. P. K. Samanata, T. Kamilya, A. K. Bhunia, "Structural and Optical Properties of Ultra-Long ZnO Nanorods", *Adv Sci Eng Med*, doi: 10.1166/asem.2016.1833, 2016.
13. P. Mitra , A. P. Chatterjee, H. S. Maiti, "ZnO thin film sensor", *Mater Lett*, doi: 10.1016/S0167-577X(97)00215-2, 1998.
14. M. Jabeen, A. Iqbal, R. V. Kumar, M. Ahmed, "Pd-doped zinc oxide nanostructures for liquefied petroleum gas detection at low temperature", *Sens Bio-Sensing Res*, doi: 10.1016/j.sbsr.2019.100293, 2019.